ChemComm

Accepted Manuscript

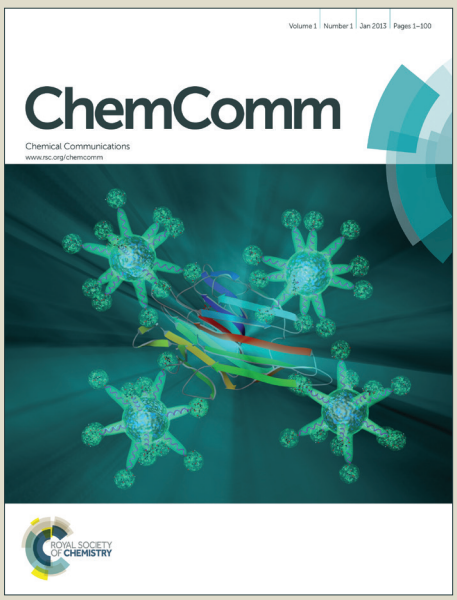

ROYAL SOCIETY OF CHEMISTRY

www.rsc.org/chemcomm

Journal Name

RSCPublishing

COMMUNICATION

Cu-nanoclusters supported on nanocrystalline SiO_2-MnO_2: a bifunctional catalyst for one step conversion of glycerol to acrylic acid†

Cite this: DOI: 10.1039/x0xx00000x

Received ooth January 2012,
Accepted ooth January 2012

DOI: 10.1039/x0xx00000x

www.rsc.org/

Bipul Sarkar,[a] Chandrashekar Pendem, [a] L. N. Sivakumar Konathala, [a] Ritesh Tiwari,[a] Takehiko Sasaki, [b] and Rajaram Bal* [a]

A highly dispersed Cu-nanoclusters anchored on nanocrystalline SiO_2-MnO_2 has been prepared and found that the material act as bifunctional catalyst for one step conversion of glycerol to acrylic acid using H_2O_2. At optimized condition a glycerol conversion of 77.1 % with 74.7% selectivity of acrylic acid was achieved after 30 h of reaction.

As the petroleum reserves are diminishing, researchers are trying to develop new ways to utilize renewable resources as the feedstock for the generation of energy and production of chemical towards lowering CO_2 emission and fossil-fuel dependency.[1] Attention has been employing for green catalytic processes to convert bio-renewable feedstock to commodity chemicals and clean fuels. Glycerol is recognized as one of the most promising building blocks for the synthesis of fine chemicals from renewable sources[2] and obtained as a by-product of different processes like soap manufacture, fatty acid production, fatty ester production, microbial fermentation [3] and transesterification or the production of biodiesel. In order to improvise the biofuel economy and put this waste stream to good use, it is necessary to develop new catalytic route to convert glycerol to value added chemicals. Thereby, development of new applications of glycerol will boost the entire glycerol industry. So the single step production of acrylic acid from glycerol will be one of the most promising options.
Acrylic acid is one of the most important chemicals and almost 4.4 million metric ton per annum global petrochemical business with average 2011 revenue of nearly $ 7 billion per year. Acrylic acid is largely employed by the chemical industry for the production of super absorber, polymer, adhesive, paint, plastic & rubber synthesis, detergent, etc. and precisely more than one billion kilograms are produced annually.[4] The entire commercial quantitative of acrylic acid is produced via two stage gas phase oxidation of propylene monomer in air. Where initially acrolein was formed, followed by oxidation of acrolein to acrylic acid. Since the propylene market price is closely tied to crude oil prices due to the use of crude oil derivatives as the feedstock for making propylene, alternative feedstock for making acrylic acid is considered to be a viable option. Various catalysts like γ-Al_2O_3, SiO_2 and TiO_2 have been applied[5] for the direct conversion of glycerol to acrolein but in most of the cases the product yield is very low. Metal oxide of Group II and Group III transition series, e.g. Nb_2O_5, WO_3/ZrO_2, metal phosphates, molecular sieves like SAPO's and zeolites have also been used for conversion of glycerol to acrolein.[6] There are few reports,[7] where two-step production of acrylic acid from glycerol have been presented. Shima et al.[7a] claimed a two-step process, which includes dehydration of aqueous solution of glycerol over alumina base catalyst to get acrylic acid yield of ~60%. Although single oxidation step conversion of glycerol to acrylic acid was reported by Jean-Luc Dubois et al [7c] using molecular oxygen over a plate heat exchanger at 250°C to 350°C, but the yield is very low. Recently, Trevisanut *et al.* and Ueda *et al.* reported the single step conversion of glycerol to acrylic acid with very poor yield.[8] Herein, we present a single step conversion of glycerol to acrylic acid over Cu-nanocluster supported on nanocrystalline SiO_2-MnO_2. The hydrothermally prepared Cu/SiO_2-MnO_2 catalyst shows the glycerol conversion of 77.1% with 74.7% acrylic acid selectivity and a TOF (turn over frequency) value of 32.9 h^{-1} was achieved. To the best of our knowledge, there is no report for the single step conversion of glycerol to acrylic acid with such high conversion and selectivity.

Cu-nanocluster supported on nanocrystalline SiO_2-MnO_2 was prepared by modifying our own preparation method (in ESI†).[9] The amount of Cu present in the catalyst was estimated by Inductively Coupled Plasma Atomic Emission Spectra (ICP-AES).It was found that 0.9 wt% Cu was present in the catalyst and the catalyst was denoted as 0.9%Cu/SiO_2-MnO_2. The powder x-ray diffraction (XRD) pattern of 0.9%Cu/SiO_2-MnO_2 catalysts is shown in Figure 1A. The standard diffraction patterns for Cu_2O and CuO are also shown as reference. All peaks for 0.9%Cu/SiO_2-MnO_2 (Figure 1A) are attributed to those of the crystalline α-MnO_2, [10] which is in accordance with

the JCPDS card, No. 44-0141. No XRD peaks attributed to either metallic Cu or its oxides has been observed for the sample 0.9%Cu/SiO_2-MnO_2, which indicates the presence of very small Cu species over the SiO_2-MnO_2 oxide surface. The morphologies of the 0.9%Cu/SiO_2-MnO_2 sample were determined by scanning electron microscope (SEM) and shown in Figure S1 B, ESI†. The SEM images of the commercial 1%Cu/SiO_2-MnO_2 is also shown in Figure S1 A, and it was found that the morphology is totally different from the hydrothermally prepared 0.9%Cu/SiO_2-MnO_2 catalyst (Figure S1 B). The SEM image shows that the particle sizes are almost uniform. The presences of Cu on SiO_2-MnO_2 support were confirmed by EDAX (energy dispersive analysis by x-ray) analysis and shown in Figure S1 C. Elemental mapping of Cu was also done, and it was found that (Figure S1 D) Cu was homogeneously distributed over SiO_2-MnO_2 support. Respective TEM images of 0.9%Cu/SiO_2-MnO_2 catalyst are shown in Figure 1A. The average particle sizes of the supported catalyst are found in between 25-50 nm. No Cu particles were imaged by HRTEM, indicating the presence of very small Cu clusters. However, the lattice fringes with a d-spacing of 3.1Å corresponding to (110) lattice plane of hexagonal α-MnO_2 are shown in Figure 1B and S2 (ESI†). The BET surface area measured by N_2 adsorption for 0.9%Cu/SiO_2-MnO_2 was 78 m^2 g^{-1}.

Figure S3B shows the $Cu_{2p3/2}$ binding energy (BE) peaks and the deconvolution of the peak shows the presence of two different types of Cu species. The BE value of 934.3 eV shows the presence of Cu^{2+} species and the peak at 932.4 eV shows the presence of either Cu^{1+} or Cu^0, as there is no difference in binding energy for Cu^{1+} and Cu^0.[11] However, from the EXAFS analysis (discussed latter) we could not found the presence of metallic Cu, so the catalyst contains Cu^{1+} not Cu^0. We have also noticed that the atomic ratio of Cu^{1+} to Cu^{2+} present in the surface is 9/1. So the surface contains mostly very small nanocluster of Cu_2O. Furthermore, the $2p_{3/2}$ binding energy value of Mn was observed at 642.2 eV along with the separation of 11.4 eV between $2p_{3/2}$ and $2p_{1/2,}$ which indicates the presence of Mn^{4+} with in the catalyst.[12,13] Figure S4 represents the TPR profile of 1%Cu/SiO_2-MnO_2^{comm} (prepared by impregnation method) and 0.9%Cu/SiO_2-MnO_2 catalyst. Three reduction peaks were observed at 236°C, 338°C and 426°C for 0.9%Cu/SiO_2-MnO_2. However, the reduction profile of 1%Cu/SiO_2-MnO_2^{comm} also shows three characteristic reduction peaks at 406 °C, 376 °C and 443°C. We believe that these three peaks are due to the following: i) reduction of Cu species (green line), ii) reduction of Mn^{4+} to Mn^{3+} (red line), and iii) reduction of Mn^{3+} to Mn^{2+} (blue line) as suggested by the literature.[14] It was also observed that the peaks shifted to lower values for the 0.9%Cu/SiO_2-MnO_2 catalyst compares to 1%Cu/SiO_2-MnO_2^{comm}. It has to be noted that, due to the presence of nanocrystalline MnO_2 particle in the 0.9%Cu/SiO_2-MnO_2 the peaks for Mn^{4+} to Mn^{2+} appeared at lower values (338 °C and 426 °C) compare to the values for commercial MnO_2 (376 °C and 443 °C). The peak due to Cu appears at 406 °C in the catalyst 1% Cu/SiO_2-MnO_2^{comm}, whereas the value shifted to 236 °C for 0.9%Cu/SiO_2-MnO_2. We attributed this peak for the reduction of very small copper oxide nanocluster.[15] It is easier to reduce the small copper oxides rather than that of the larger particle present in the bulk due to diffusion limitation.[16] So the size of the copper oxide particle is smaller in 0.9%Cu/SiO_2-MnO_2 compare to the bulk 1%Cu/SiO_2-MnO_2^{comm}. Commercial MnO_2 do not show any acidity, however SiO_2 shows weak acid sites (Figure S5 A-C; ESI†) but the as prepared Cu/SiO_2-MnO_2 catalyst shows moderate acidity of 149 μmol g^{-1}. We believe that the enhancement of surface acidity is mainly due to the presence of nanocrystalline SiO_2 along with hexagonal MnO_2 (as confirmed by TEM analysis Figure S2, ESI†). Earlier reports also revealed that hexagonal MnO_2 are responsible for the generation of acid sites.[17] So the total acidity arise due to the presence of SiO_2 and hexagonal MnO_2 in the catalyst. NH_3-TPD pattern of the Cu/SiO_2-MnO_2 (Figure S4, ESI†) shows a broad peak spanning between temperature 200-320°C Deconvolution of the peak shows the presence of two peaks and we assume that the first peak is due to the presence of SiO_2 and the second peak is due to the presence of hexagonal MnO_2 in the catalyst. It is very clear from the TPD spectra that the second peak is bigger than the first peak, which clearly indicates that the enhancement of the acidic sites is mainly due to the formation of hexagonal MnO_2. The Cu-XANES spectra of the Cu/SiO_2-MnO_2 for the fresh and spent catalyst are shown in Figure S6 (ESI†); for comparison the XANES spectra of Cu foil, commercial Cu_2O, CuO are also presented. It is well known for the Cu^{1+} compound that they exhibit as two peaks due to the transition of $1s \rightarrow 4p_{x,y}$ at 8984 eV and $1s \rightarrow 4p_z$ at 8995 eV.[18] While metallic Cu and Cu^{1+} have no hole in the 3d orbital but Cu^{2+} compound are in a d^9 configuration shows a weak pre-edge peak representing the quadrapole allowed $1s \rightarrow 3d$ transition appears below the edge. The XANES spectra of the 0.9%Cu/SiO_2-MnO_2 catalyst, which are not typical of Cu_2O but more likely to be associated with mixture of Cu_2O and CuO.

Detail structural parameters of the Cu species were obtained by Cu k-edge EXAFS analysis. The K^3-weighted Fourier Transformation of Cu-K edge EXAFS spectra are shown in Figure S7. The curve fitting result are summarized in the Table S1. The spectra cannot be fitted as either pure CuO crystal or Cu_2O crystal. It is a small crystal of Cu_2O with dispersed CuO. The EXAFS spectra of 0.9%Cu/SiO_2-MnO_2 fresh (Figure S7A) and spent catalyst (Figure S7B) shows the presence of small crystals of Cu_2O with dispersed CuO. For the fresh catalyst, the Cu-O bond length of 1.954±0.152Å with CN 1.9±0.7 indicates the presence of Cu^{2+} species. The copper oxide nanoclusters over SiO_2-MnO_2 were durable under glycerol oxydehydration reaction. The structure parameters determined by Cu k-edge EXAFS for 0.9%Cu/SiO_2-MnO_2 after the glycerol oxydehydration indicates that there is no significant change in the structure of the nanocluster after 30h reaction (spent catalyst, Table S1). The Cu-O bond length of 1.951±0.113Å with CN of 1.7±0.6 shows that the nanoclusters size is almost same even after the reaction. Furthermore, EXAFS analysis confirms that there was no Cu-Cu bond present in the catalyst. This clearly indicates that Cu^o (metallic cupper) is not present in our catalyst

The activities of the different Cu-catalysts are shown in Table 1. Oxydehydration of glycerol over 0.9%Cu/SiO_2-MnO_2 catalyst shows acrylic acid and acrolein as the main product with the formation of small amount of 3-hydroxypropionaldehyde. A glycerol conversion of 77.1% with 74.7% acrylic acid selectivity (entry 4) was achieved over 0.9%Cu/SiO_2-MnO_2 catalyst after 30h of reaction with a TOF (turn over frequency) value of 32.9 h^{-1}. Commercial MnO_2 shows (entry 1) only 5.5% glycerol conversion without any formation of acrylic acid. 1%Cu supported on SiO_2-MnO_2 (prepared by physical mixing) also shows negligible selectivity for acrylic acid (entry 3). MnO_2 prepared by the hydrothermal

method also showed low activity (8.6% conversion and 5.6 % acrylic acid selectivity, entry 2). Cu supported on MnO_2 or SiO_2 (entry 7&8) also does not show any activity. So the presence of Cu nanoclusters and the presence of acid sites (due to SiO_2 and MnO_2) are the key factors for the oxydehydration of glycerol. A probable mechanistic pathway for the formation of acrylic acid is shown in the scheme 1. The catalyst behaves as a bifunctional catalyst, where presence of SiO_2 and hexagonal MnO_2 sites acts as an acidic site responsible for dehydration reaction (glycerol to acrolein) and Cu^+ sites are responsible for oxidation reaction (acrolein to acrylic acid). Based on the result obtained we believed that the reaction goes through at least two intermediates: 3-hydroxypropionaldehyde and acrolein. Where the first step is the dehydration of glycerol to form of 3-hydroxypropionaldehyde over the acid site of the catalyst. The second step also the dehydration of the 3-hydroxypropionaldehyde to form acrolein. Finally acrolein oxidizes to form acrylic acid in presence of H_2O_2 (50% in H_2O) over Cu sites. To check the intermediate acroline formation, we did the experiment taking the acrolein as the substrate and found that both acrolein conversion and acrylic acid selectivity was 100% within 3h (entry 6). We believe that the dehydration step is very slow, but the oxidation step is very fast. Initially it takes large time to form acrylic acid. But once acrylic acid formation begins it act as Brösted acid in the reaction mixture and the rate of acrylic acid formation increases. The increase in the H_2O_2: glycerol (Figure S8, ESI†) molar ratio does not have any substantial effect on acrylic acid selectivity, as it remains almost same. A noticeable increase in glycerol conversion from 49.9% to 77.1% was observed on going from glycerol to H_2O_2 molar ratio of 2.5 to 5; whereas conversion decreases from 77.1% to 70.1% with the further increase in glycerol to H_2O_2 molar ratio of 7.5. It seems with the increase in H_2O_2 mole ratio the decomposition of H_2O_2 increases, so the glycerol conversion decreases. The effects of temperatures are shown in Figure 2A. It was found that the glycerol conversion increases continuously with temperature but the selectivity decreases above 70°C. We believe that above 70°C the decomposition of H_2O_2 taking place, so the selectivity decreases. The effect of reaction time is shown in Figure 2B. It was observed that both the glycerol conversion and acrylic acid selectivity continuously increasing when the reaction time was increased from 10 to 30h but the selectivity decreased after 30h.

The reusability of the catalyst 0.9%Cu/SiO_2-MnO_2 was studied without any regeneration. The catalyst showed almost same activity even after four successive run in same reaction condition. The catalyst showed 72.8% conversion and 72.1% acrylic acid selectivity after 4 recycle (entry 5, Table 1). The small decrease in the activity could be mainly due to unavoidable loss of the catalyst during washing. The ICP-AES analysis of fresh and spent catalyst after four successive reuse confirms no leaching of Cu metal from the catalyst, which also supporting the true heterogeneity of the catalyst.

Scheme 1. Probable mechanistic pathway for the conversion of glycerol to acrylic acid.

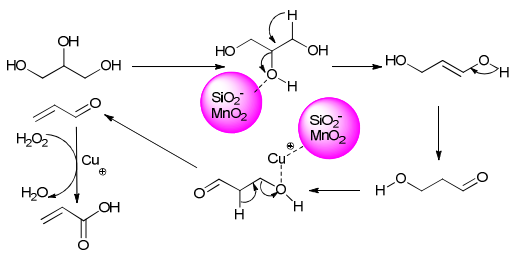

Figure 1. (A) X-ray diffraction patterns of commercial CuO, Cu_2O, MnO_2 and prepared 0.9%Cu/SiO_2-MnO_2. (B) TEM images of prepared 0.9%Cu-SiO_2-MnO_2 (a) low magnification and (b) high magnification.

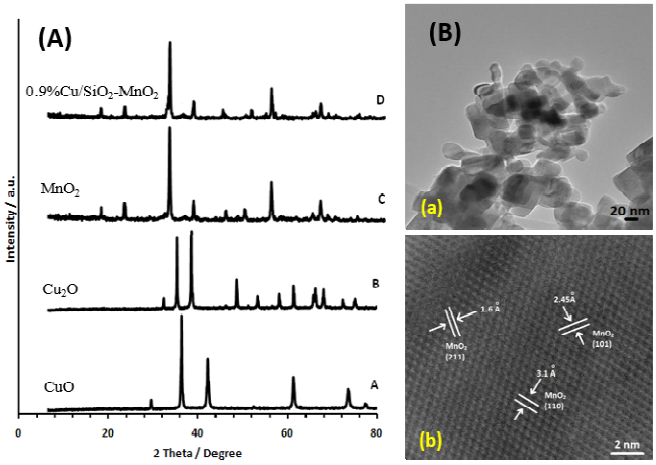

Figure 2. (A) Effect of reaction temperature and (B) the effect of reaction time (h) as the function of glycerol oxidation with 0.046g catalysts, 0.92g glycerol in 10 ml solvent were stirred at 70°C. [■] Glycerol conversion; [●] Selectivity to acrylic acid; [▼] Selectivity to acrolein and [▲] Selectivity to 3HPA.

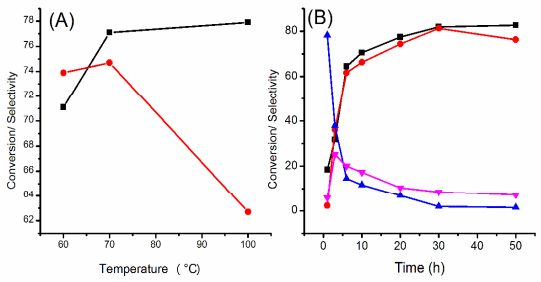

Table 1. Activity of the Cu/SiO_2-MnO_2 catalyst.

Sl No	Catalyst	χ_G (%)[c]	Selectivity (C %)				TOF (h^{-1})	E_o
			AA	3HPA	AC	OT		
1	MnO_2[com]	5.5	0.1	2.8	3.1	~94.0	-	~0
2	MnO_2	8.6	5.6	2.5	1.8	~90.1	-	0.09
3	1%Cu/SiO_2-MnO_2[com]	9.7	3.4	3.0	3.5	90.1	-	0.06
4	0.9%Cu/SiO_2 -MnO_2	77.1	74.7	6.8	10.4	8.1	32.9	11.52
5	0.9%Cu/SiO_2 -MnO_2[a]	72.5	72.0	5.8	11.6	10.6	30.7	10.52
6	0.9%Cu/SiO_2 -MnO_2[b]	100	100	-	-	-	-	20.0
7	1%Cu/MnO_2	8.3	0	4.1	4.8	91.1	-	-
8	1%Cu/SiO_2	7.7	0	3.7	12.9	83.4	-	-

Catalysts: 0.046 g; glycerol: 0.92 g in 10 mL CH_3CN, temperature: 70°C; substrate (glycerol): 50% H_2O_2 (1:5, mole ratio). [com] commercial oxide. [a] after 4 successive run in same condition; [b] with acrolein as substrate after 3 h reaction; [c] in mol %. TOF: Moles of acrylic acid produced per moles of Cu per unit time; E_O: H_2O_2 efficiency calculated by (100 x moles of acrylic acid formed) / total moles of H_2O_2 added; C balance was carried out for most of the experiments and the value was within 98-102%. χ_G =conversion of glycerol (C%), AA= Acrylic acid, AC=Acrolein and OT=others.

Conclusions

In summary, we have found Cu nanoclusters supported on SiO_2-MnO_2 was found to be a very efficient catalyst for direct conversion of glycerol to acrylic acid using hydrogen peroxide as oxidant. A glycerol conversion of 77.1 % with 74.7% acrylic acid selectivity was achieved after 30 h of reaction. The Cu species could not be detected by XRD or TEM but the EXAFS study revealed the formation of Cu-nanoclusters on the MnO_2 support. Cu-nanoclusters and nanocrystalline SiO_2-MnO_2 is the key parameter for high conversion and selectivity in oxydehydration of glycerol. The reusability of the catalyst was tested by conducting 4 successive run with the same catalyst. The catalyst showed similar glycerol conversion with same acrylic acid selectivity confirming the true reusability of the catalyst.

Acknowledgements

B. S. acknowledges University Grant Commission (UGC), India for the fellowship. We also acknowledge Director CSIR-IIP for his support. The authors thank Analytical Science Division, Indian Institute of Petroleum for analytical services. The XAFS measurements were performed at KEK-IMSS-PF with the approval of the Photon Factory Advisory Committee (project 2010G109).

Notes and references

[a] Catalytic Conversion & Processes Division
CSIR-Indian Institute of Petroleum
Dehradun 248005, India
Tel.: +91 135 2525797; Fax: +91 135 2660202
E-mail: raja@iip.res.in
[b] Prof. T. Sasaki
Department of Complexity Science and Engineering
The University of Tokyo
Kashiwanoha, Kashiwa-shi, Chiba 277-8561, Japan
† Electronic Supplementary Information (ESI) available: See DOI: 10.1039/b000000x/

1. (a) W. S. Broecker, T. Takahashi, H. J. Simpson and T. H. Peng, *Science,* 1979, **206**, 409; (b) P. D. Quay, B. Tilbrook and C. S. Wong, *Science,* 1992, **256**, 74; (c) S. Dahl and I. Chorkendorff, *Nature Materials,* 2012, **11**, 100.
2. (a) C. H. Zhou, J. N. Beltramini, Y. X. Fan and G. Q. Lu, *Chem. Soc. Rev.,* 2008, **37**, 527; (b) F. Jerome, Y. Pouilloux and J. Barrau, *ChemSusChem,* 2008, **1**, 586; (c) A. Corma, S. Iborra and A. Velty, *Chem. Rev.,* 2007, **107**, 2411; (d) G. W. Huber, R. D. Cortright and J. A. Dumesic, *Angew. Chem. Int. Ed.,* 2004, **43**, 1549; (e) G. W. Huber, J. W. Shabaker and J. A. Dumesic, *Science,* 2003, **300**, 2075.
3. Glycerol, in *Kirk-Othmer Encyclopedia of Chemical Technology*, John Wiley & Sons, Inc., New York 2001.
4. (a) S. H. Lee, S. J. Park, O. J. Park, J. Cho and J. W. Rhee, *J Microbiol & Biotechnol,* 2009, **19**, 474; (b) S. Kudla and M. Kaledkowska, *Przemysl Chemiczny,* 1998, **77**, 86; (c) P. A. Glubish, *Use of Polymers of Acrylic Acid and Its Derivatives in the Textile and Light Industries,* 1975**,** pp. 205; (d) P. C. Chromecek, W. G. Deichert, J. J. Falcetta and M. F. VanBurn, *US pat., 4276402*, 1981.
5. (a) Y. T. Kim, K. D. Jung and E. D. Park, *Appl. Catal. B*, 2011, **107**, 177; (b) E. Tsukuda, S. Sato, R. Takahashi and T. Sodesawa, *Catal. Commun.,* 2007, **8**, 1349.
6. (a) S. H. Chai, H. P. Wang, Y. Liang and B. Q. Xu, *J. Catal.,* 2007, **250**, 342; (b) A. Ulgen and W. Hoelderich, *Catal. Lett.,* 2009, **131**, 122; (c) W. Suprum, M. Lutecki, T. Haber and H. Papp, *J. Mol. Catal. A,* 2009, **309**, 71; (d) Y. T. Kim, K. D. Jung and E. D. Park, *Microporous Microporous Mater.,* 2010, **131**, 28; (e) A. Corma, G. W. Huber, L. Sauvanaud and P. O'Connor, *J. Catal.,* 2008, **257**, 163.
7. (a) M. Shima, K. Shi and T. Takahashi, *EU pat., EP1710277B1*, 2005; (b) J. L. Dubois, *Pat. App. No, 20100168471 (AC07C5116FI)*, 2010; (c) J. L. Dubois, C. Duquenne and W. Holderich, *US Pat., 7910771*, 2011; (d) S. H. Chai, H. P. Wang, Y. Liang and B. Q. Xu, *Green Chem.,* 2008, **10**, 1087.
8. (a) M. D. Soriano, P. Concepcion, J. M. L. Nieto, F. Cavani, S. Guidetti and C. Trevisanut*, Green Chem.,* 2011, **13**, 2954; (b) F. Wanga, J. L. Duboisb and W. Ueda, *J. Catal.,* 2009, **268**, 260.
9. (a) B. Sarkar, P. Prajapati, R. Tiwari, R. Tiwari, S. Ghosh, S. S. Acharyya, C. Pendem, R. K. Singha, L. N. S. Konathala, J. Kumar, T. Sasaki and R. Bal, *Green Chem*., 2012, **14**, 2600; (b) S. S. Acharyya, S. Ghosh, R. Tiwari, B. Sarkar, R. K. Singha, T. Sasaki, C. Pendem and R. Bal, *Green Chem.,* 2014, **16**, 2500.
10. Z. Y. Yuan, Z. Zhang, G. Du, T. Z. Ren and B. L. Su, *Chem. Phys. Lett.,* 2003, **378**, 349.
11. C. D. Wagner, A. V. Naumkin, A. K. Vass, J. W. Allison, C. J. Powell and J. R. Jr. Rumble, *NIST Standard Reference Database 20, Version 3.4 (web version) (http:/srdata.nist.gov/xps/)* 2003.
12. (a) A. A. Mirzaei, H. R. Shaterian and M. Kaykhaii, *Appl. Surf. Science,* 2005, **239**, 246; (b) H. Y. Chen, J. Lin, K. L. Tan and J. Li, *Appl. Surf. Science* 1998, **126**, 323; (c) F. Marquez, A. E. Palomares, F. Rey, and A. Corma, *J. Mater. Chem.,* 2001, **11**, 1675; (d) M. Diab, B. Moshofsky, I. J. La-Plante and T. Mokari, *J. Mater. Chem.,* 2011, **21**, 11626.
13. C. D. Wagner, W. M. Riggs, L. E. Davis, J. F. Moulder and G. E. Muilenberg, *Handbook of X-ray Photoelectron Spectroscopy, Perkin-Elmer Corp., Eden Prairie*, USA, 1979.
14. S. Liang, F. Teng, G. Bulgan, R. Zong and Y. Zhu, *J. Phys. Chem. C,* 2008, **112**, 5307.
15. Z. Ma, Z. Xiao, J. A. van Bokhoven and C. Liang, *J. Mat. Chem.,* 2010, **20**, 755.
16. R. Rajeev, K. A. Devi, A. Abraham, K. Krishnan, T. E. Krishnan, K. N. Ninan and C. G. Nair, R. *Thermochim. Acta,* 1995, **254**, 235.
17. Z. R. Tian, W. Tong, J. Y. Wang, N. G. Duan, V. V. Krishnan and S. L. Suib, *Science,* 1997, **276**, 926.
18. (a) J. Y. Kim, J. A. Rodriguez, J. C. Hanson, A. I. Frenkel and P. L. Lee, *J. Am. Chem. Soc.,* 2003, **125**, 10684; (b) W. B. Kim and J. S. Lee, *J. Phys. Chem. B,* 2003, **107**, 9195.

